Jurnal Geografi, Edukasi dan Lingkungan (JGEL) Vol. 8, No. 2, Juli 2024:111-126
P-ISSN: 2579–8499; E-ISSN: 2579–8510
Doi: https://doi.org/10.22236/jgel.v8i2.13128
Website: http://journal.uhamka.ac.id/index.php/jgel

Spatio-Temporal Analysis Of Yogyakarta Internasional Airport Development Impact On LULC And LST In Kulon Progo

Agung Jauhari[1*], Dwi Setyo Aji[1], Ilham Kio Hafidz[1], Aldea Rizka Novareka[1,2], Dwika Ajeng Oktaviani[1], Aditya Rico Oktavian[1]
[1]Department of Earth Technology, Vocational College, Universitas Gadjah Mada, Yogyakarta, Indonesia
[2]Geography Study Progam, Faculty of Geography, Universitas Muhammadiyah Surakarta, Surakarta, Indonesia

***E-mail:** agungjauhari@ugm.ac.id
Received: 10 11 2023 / *Accepted*: 17 05 2024 / *Published online*: 18 07 2024

ABSTRAK

Pembangunan Bandara Internasional Yogyakarta (YIA) diyakini akan memicu perkembangan wilayah secara masif di Kabupaten Kulon Progo, baik untuk pengembangan infrastruktur maupun fasilitas pendukungnya. Konversi lahan bervegetasi lebat menjadi lahan terbangun, diperkirakan akan meningkatkan Suhu Permukaan Tanah (LST). Penelitian ini bertujuan untuk mempelajari perubahan spasio-temporal penutup dan penggunaan lahan dan LST di Kabupaten Kulon Progo. Data yang digunakan yakni Landsat 8 pada tiga periode, yaitu sebelum pembangunan (2013), pada awal pembangunan (2017), dan setelah YIA beroperasi penuh (2021). Pola spasial LST diselidiki menggunakan statistik spasial, yakni Global Moran's I untuk mengidentifikasi ada tidaknya autokorelasi dan Hot Spots Analysis (Getis-Ord G) untuk menganalisis pola sebaran. Hasil kajian menunjukkan sejak pembangunan YIA, luas lahan terbangun dan lahan terbuka meningkat secara signifikan (menjadi empat kali lipat), sementara lahan pertanian berkurang 14% setelah (2017-2021). Pola sebaran LST berkaitan erat dengan jenis penutup dan penggunaan lahan, yakni LST tinggi terletak pada Lahan Terbangun dan Lahan Terbuka (32 ºC -38ºC), sedangkan LST yang lebih rendah terletak pada lahan Hutan (27ºC-31ºC). Kemudian, Indeks Moran's I pada tiga periode waktu menunjukkan nilai sekitar 0.9 (mendekati 1) yang menunjukkan adanya autokorelasi spasial positif. Nilai p-value (0.00) juga secara signifikan menunjukkan LST membentuk pola mengelompok. Analisis Klaster Spasial, Hot Spot Analysis (Getis-Ord Gi*) juga menunjukkan bahwa terdapat klaster area dengan suhu tinggi (hot spot) yakni di sepanjang pesisir dan area perkotaan, sedangkan area dengan suhu rendah (cold spot) juga mengelompok di sekitar Perbukitan Menoreh.*

Kata Kunci: *Bandara Internasional Yogyakarta, Penutup dan Penggunaan Lahan, Suhu Permukaan Lahan, Statistik Spasial*

ABSTRACT

Yogyakarta Internasional Airport (YIA) development is predicted to trigger massive development in Kulon Progo Regency, whether for the infrastructure or supporting facilities development. Land conversion from densely vegetated land into less dense vegetated land, i.e., forest or garden to built-up areas, is determined to increase Land Surface Temperature (LST). This research studied the spatiotemporal change of LULC and LST change in Kulon Progo Regency by employing Landsat 8 data for three periods respectively, before the development (2013), at the start of construction (2017), and after the YIA fully operated (2021). The spatial pattern of LST was also investigated using spatial statistics, namely, Global Moran's I, to identify spatial autocorrelation and Hot Spots Analysis (Getis-Ord G*) to determine the spatial patterns or clusters. The findings showed that since the YIA development, the built-up area and bare land

increased significantly (quadruple), while agriculture reduced dramatically by 14%. Furthermore, the LST was closely related to the LULC, where the high LST was located in the built-up area and bare land (32 ºC -38ºC), while the low LST was located in the forest (27ºC-31ºC). Moran's I index, around 0.9 (close to 1), indicates a positive spatial autocorrelation, while the p-value (0.00) indicates that the LST was significantly clustered. Indeed, Hot Spot Analysis (Getis-Ord Gi*) revealed that the high-temperature areas clustered (hot spot) along the coastal and urban areas, while low-temperature areas clustered around Menoreh Hills.

Keywords: Yogyakarta Internasional Airport; LULC, Land Surface Temperature, Spatial Statistics

INTRODUCTION

The development of Yogyakarta Internasional Airport (YIA) in Kulon Progo Regency intends to stimulate economic growth and develop the infrastructure along with the socio-economic condition of the local communities (Ayuningtyas, 2022). The government also attempted to reduce inequality and simultaneously develop Kulon Progo Regency as well as surrounding areas by establishing new infrastructures.

Economic development is often considered a factor behind the rapid urban expansion and environmental problems. Many countries once boosted economic growth and large-scale investment by sacrificing environmental and social aspects, resulting in environmental degradation, the loss of agricultural land, higher poverty and inequality, and local livelihoods transition (Ha et al., 2020; Ochoa et al., 2018; Zoomers & Otsuki, 2017).

Developing new infrastructures is widely known for initiating LULC conversion and promoting built-up areas for infrastructure construction or following development, i.e., settlements, commercial and industrial areas (Bamrungkhul & Tanaka, 2022; Rustiadi et al., 2021). Yogyakarta's urban area has transformed rapidly due to the development of urban infrastructures, settlements, and commercial property, which will likely trigger more farmland loss in the upcoming decade (Widodo et al., 2015).

The LULC change is highly contributed to modifying the environmental elements, for instance, the urban thermal environment (Naikoo et al., 2020). Moreover, converting vegetated land into built-up areas significantly affects the surging of land surface temperature, an essential problem in the urban area (Singh et al., 2017). Hence, the airport development in Kulon Progo Regency is projected to prompt massive land conversion for developing other facilities, i.e. hotels, shops, restaurants, and service centres.

As the representation of the Earth's top surface, LULC is decisive on the state of Earth's radiative temperature (Kumari et al., 2019) since the behaviour of each LULC type is varied to solar radiation. Land surface temperature is often measured to describe surface urban heat islands (SUHI), while air temperature is describe atmospheric urban heat islands (EPA, 2011; Estoque et al., 2017).

The Earth's surface temperature measurement can be determined by field survey or remote sensing data observation. Krishnan et al. (2015) compare the LST data from satellite imagery (MODIS), aircraft measurement and infrared temperature sensors; Sam & Balasubramanian (2023) employed MODIS to detect the LST in Kanyakumari district, India; Njoku & Tenenbaum (2022) used Landsat 7 and Landsat 8 to investigate the LST in Ilorin, Nigeria; while Nugraha et al. (2019) also used Landsat 7 and Landsat 8 to derive LST for

analyse drought monitoring in East Jawa, Indonesia.

Since Earth's temperature affects the climate, weather, and quality of human life, monitoring LST is critical. Several studies on LST or SUHI have been conducted in Yogyakarta, mainly focusing on the Yogyakarta Urban Area or Yogyakarta City, such as Pratiwi et al. (2018) studied the relationship between LST and green infrastructure planning in Yogyakarta City; Atianta (2020) identified the relationship between land utilisation intensity and LST in Yogyakarta urban area; Arrofiqoh & Setyaningrum (2021) analysed the LST during Covid-19 pandemic in Yogyakarta urban area while Nando (2021) studied the similar topic in Kediri City, East Java; and Prastyo et al. (2022) examined the distribution of SUHI in settlements area in Yogyakarta city.

However, studies related to the impact of new infrastructure development on LST are limited. Kumari et al. (2019) studied the impact of thermal power plant development on LST in India. Even with this, the further impact of thermal power plant development in generating urban expansion is considered less significant compared to urban infrastructure, i.e. airports, education facilities, and industries.

Since research concerning the impact of YIA on urbanisation is still limited, this study intends to examine the spatio-temporal change of land urbanisation and its consequences on LST in Kulon Progo Regency. Urbanisation was identified from LULC changes, while LST was estimated from remote sensing thermal data, which both were derived from Landsat 8 imagery using Google Earth Engine (GEE). As a cloud-based platform, GEE offers access to large geospatial datasets and high-performance computation without the high-end hardware to store and handle the data locally (Liang et al., 2020).

In short, the objectives of this research are (1) to study the spatiotemporal change of LULC and LST change in Kulon Progo Regency and (2) to investigate the spatial pattern of LST and its relations to LULC. The analysis focused on three points of time: before the development (2013), at the start of the construction (2017), and after the airport officially operated (2021). Spatial statistics analysis with Global Moran's I and Getis-Ord Gi* Hot Spot Analysis were used to visualize the spatial autocorrelation and illustrate the spatial pattern of LST. Hopefully, this research will help policymakers and scientists in urban development studies to evaluate the impact of infrastructure development based on spatial data.

METHODS

Study Area

Kulon Progo Regency, as the study area, is located in the western part of Yogyakarta Special Province, Indonesia. The region lies between the latitudes 7º38'42" S and 7º59'3" S and the longitudes 110º1'37" E and 110º16'26" E, which is approximately ± 40 km of the Yogyakarta Urban Area (**Figure 1**). The area coverage is 58,627.51 ha, consisting of 12 districts, where the YIA is located in Temon District on the southwest coast of the regency.

According to the Statistical Bureau of Kulon Progo, in 2022, the total population of Kulon Progo regency is 451,342 people. The population density is 770 people per square kilometre, while Wates District, the capital regency, has the highest density with 1,523 people per square kilometre (Statistical Bureau of Kulon Progo Regency, 2023). Kulon Progo Regency is also often considered an underdeveloped region compared to other regions in Yogyakarta. As a piece of evidence, the poverty rate in 2021 was 18.38%, which is the highest in Yogyakarta, with an average of 11.91%

and even higher than the National poverty rate (9.71%) (Nugraha et al., 2022).

In general, the topographical profile of Kulon Progo Regency can be divided as follows: the north part is highlands, as part of Menoreh Hill, with an elevation of 500-1,000 meters AMSL; hills with an elevation of 100-500 metres AMSL the middle area, and plains area in the south are mostly the coastal areas with elevation less than 100 meters AMSL (Statistical Bureau of Kulon Progo Regency, 2023). It is understood that the topographical condition in the middle and northern areas of the regency also contributes to the abate of the development in this region.

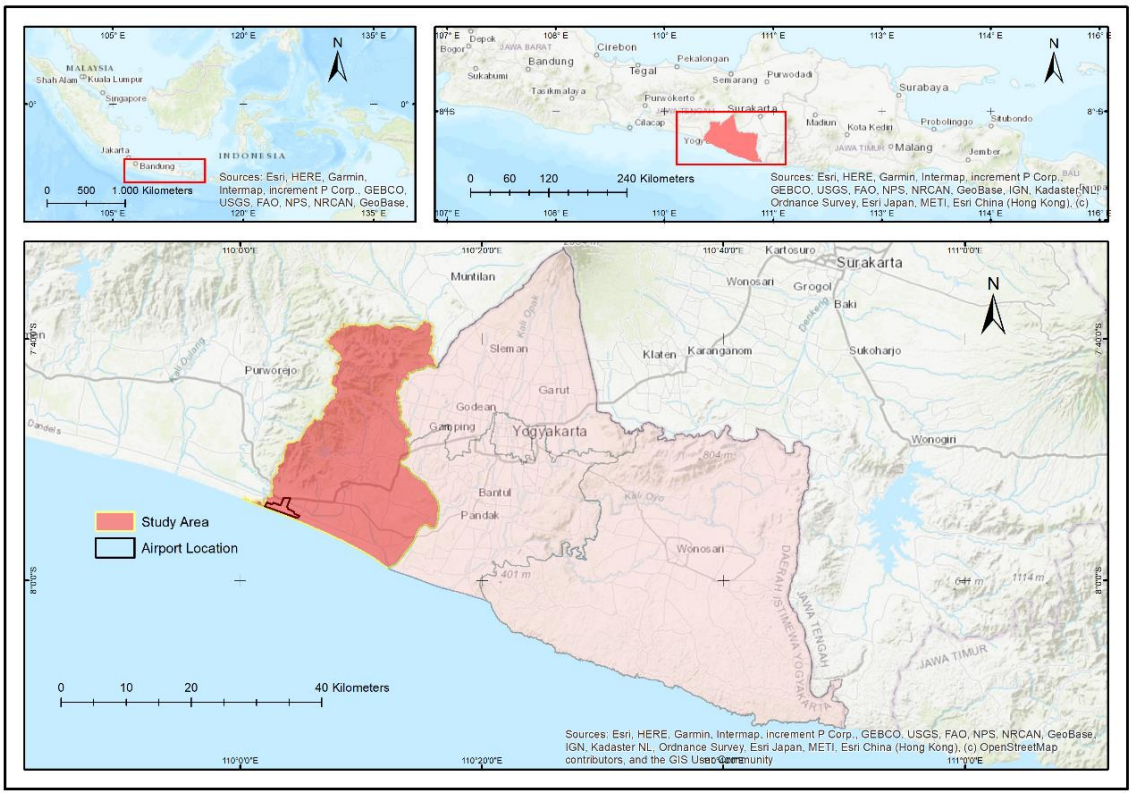

Figure 1. The study area, Kulon Progo Regency

The policy to develop a new airport area is, also believed, an agenda to generate urbanisation and development in the western part of Yogyakarta and its surroundings, both physical and economic aspects. Moreover, in response to the YIA development in 2017, the local government launched the "Bedah Menoreh" programme, which intends to expand accessibility and develop economically promising resources. The program focused on developing connectivity between YIA and Borobudur Temple, considered a super-priority tourism destination, through Menoreh Hill (RPJMD Kabupaten Kulon Progo Tahun 2017-2022, 2017).

The area around Menoreh Hills, previously known as an isolated area due to the topographical condition and lack of accessibility, will be unlocked and potentially grow as a new development centre. The government intends to develop local tourism destinations and promote the featured products to generate local and regional economic advancement. The multiple economic policies and infrastructure development will likely

boost the urbanisation and regional development in Kulon Progo Regency.

Data collection techniques

This research focuses on analysing the spatial change of urban LULC as a response to the development of Yogyakarta Internasional Airport in Kulon Progo Regency, Yogyakarta Special Province, Indonesia. Google Earth Engine (GEE) was used to select the cloud-free satellite Imagery of Landsat 8 to obtain the LULC and LST maps. The Landsat 8 OLI satellite imagery data with a resolution of 30 meters acquired for 2013, 2017, and 2021 represent three periods, namely before, during, and after the development of the airport. The code is available here: https://code.earthengine.google.com/?accept_repo=users/agungjauhari/LULC_LST_YIA. Hence, the study area boundary or administration boundary of Kulon Progo Regency was acquired from the geoportal website, which can be accessed through http://geoportal.kulonprogokab.go.id/.

LULC classification

The land use and land cover in the study area was classified into seven (7) classes (**Table 1**). The classification method modified LULC classification from Saputra & Lee (2019), which also employed Landsat 8 series as the data source to create LULC maps in North Sumatra, Indonesia, despite selected classes only that have similarities in the study area.

Table 1. LULC Classification

No.	Classification	Description
1	Agriculture	The area for crop plants, both dry-land and wet-land
2	Bareland	The barren or open area
3	Built up	The built area, i.e. residentials, airports, commercials, etc.
4	Forest	The area of plantation forest or community forest
5	Garden	The vegetated area near the settlement
6	Shrub	Area with shrub and juvenile plant area
7	Water	Area covered by water, i.e. reservoirs, rivers, lakes, etc.

Source: modified from Saputra & Lee (2019)

LST estimation

Land Surface Temperature in this research was extracted from Landsat 8 imagery. The Split Window Algorithm (SWA) method is often used to estimate the LST by normalising the thermal band, namely, Band 10 and Band 11, to produce optimal LST value (Indrawati et al., 2020; Nugraha et al., 2019). There are steps to acquire LST from Landsat 8 such as follows (Latif, 2014; Pratiwi et al., 2018):

Step 1: Estimation of ToA Spectral Radiance of TIRS and OLI Sensors using formula 1.

$$L\lambda = \left(\frac{L_{max}-L_{min}}{DN_{max}}\right) * Band + L_{min} \quad .....(1)$$

where $L\lambda$ ToA spectral radiance in watts, L_{max} maximum radiance respective band, L_{min} the minimum radiance of respective band, and DN_{max} the difference between max and min calibration of sensors

Step 2: Estimate the Brightness Temperature of Band 10 and Band 11 using formula 2.

$$T_b = \frac{K2}{log\left(1 + \frac{K1}{L\lambda}\right) - 273{,}15} \quad .....(2)$$

where *K1* and *K2* are thermal constants of bands, $L\lambda$ the ToA spectral radiance layer.

Step 3: Calculate the NDVI using formula 3.

$$NDVI = \frac{BAND5 - BAND4}{BAND5 + BAND4} \quad \text{.....(3)}$$

Range of NDVI: - 1 <NDVI < +1

Step 4: Estimate the Fractional Vegetation Cover (FVC) using formula 4.

$$FCV = \frac{NDVI - NDVIsoil}{NDVIveg - NDVIsoil} \quad \text{.....(4)}$$

where FVC is Fractional Vegetation Cover), NDVI (normalized different vegetation indices), NDVIsoil is NDVI on soil, and NDVIveg is NDVI on vegetation.

Step 5: Estimate the Land Surface Emissivity (LSE) using formula 5.

$$LSE = \varepsilon_s * (1 - FCV) + e_v * FVC \quad \text{...(5)}$$

where FCV is fractional vegetation cover, ε_s emissivity of soil, ε_v emissivity of vegetation

Step 6: Mean and difference of LSE using formula 6-8.

$$Mean\ of\ LSE = \varepsilon = \frac{LSE10 + LSE11}{2} \quad \text{.....(6)}$$

$$Difference\ of\ LSE = \Delta\varepsilon = LSE_{10} - LSE_{11} \quad \text{.....(7)}$$

Step 7: Estimation of LST

$$LST = TB_{10} + C_1(TB_{10} - TB_{11}) + C_2(TB_{10} - TB_{11})^2 + C_0 + (C_3 - C_4W)(1 - m) + (C_5 + C_6W)\Delta \quad \text{.....(8)}$$

where $TB_{10}\ and\ TB_{11}$ are the brightness temperature of Band 10 and Band 11, $C_0 - C_6$ are split window coefficient, ε mean LSE, $\Delta\varepsilon$ margin of LSE, w is atmospheric water-vapour content (0.013).

Spatial autocorrelation and cluster analysis

Based on Tobler's (1979) first law of geography: "every feature is related to each other, but the near objects are related closer than father objects". Spatial statistics often used by scientist to analysed the spatial pattern of geospastial data, i.e. Kumari et al. (2019) analysed LST pattern using Moran's I statistics, Li et al. (2019) also employ Moran's I statistics to analysed the spatial pattern of land use conversion in China, Dahlia (2021) employ spatial autocorrelation to studied the spatial pattern of Covid-19 cases in Jakarta, and Punzo et al., (2022) analysed the land consumption in Italy using Moran's I and Geographically Weighted Regression.

In this study, spatial autocorrelation utilised to evaluate the spatial pattern of LST in the study area due to LULC changes. Pradhan et al. (2017) described that urban LULC pattern mostly has strong relationships with urban growth, potentially affecting LST. Spatial autocorrelation (SA) represents a relationship between nearby spatial units, where each unit is coded with a realization of a single variable (Fischer & Getis, 2010). The spatial autocorrelation using Moran's I statistics was calculated from ESRI GIS software based on the following formulas 9 -13 (ESRI, 2023b):

$$I = \frac{n}{S_0} \frac{\sum_{i=1}^{n}\sum_{j=1}^{n} w_i, z_i z_j}{\sum_{i=1}^{n} z_i^2} \quad \text{.....(9)}$$

z_i : presents the deviation of the value of i from the mean of $(x_i - X)$

$w_{i,j}$: spatial weight of i and j

n : number of features

So : All spatial weights aggregate

where,

$$S_0 = \sum_{i=1}^{n}\sum_{j=1}^{n} w_{i,j} \quad \text{.....(10)}$$

On the other hand, z_I-score for the statistics calculated as follows:

$$z_I = \frac{I - E[I]}{\sqrt{V[I]}} \quad \text{.....(11)}$$

where,

$$E[I] = \frac{-1}{(n-1)} \quad \text{.....(12)}$$

$$V[I] = E[I^2] - E[I]^2 \quad \text{.....(13)}$$

Further analysis beyond spatial autocorrelation is cluster analysis, which is also essential to describe the pattern of LST in the study area. Hot Spot Analysis using Getis-Ord Gi* can be performed to identify the spatial clusters of hot spots (high values) and cold spots (low values). The formulas 14-16 are as follows (ESRI, 2023a):

$$G_i^* = \frac{\sum_{j=1}^{n} w_{i,j}\, x_j - \bar{X}\sum_{j=1}^{n} w_{i,j}}{s\sqrt{\frac{\left[n\sum_{j=1}^{n} w_{i,j}^2 - \left(\sum_{j=1}^{n} w_{i,j}\right)^2\right]}{n-1}}} \quad \text{.....(14)}$$

x_j : presents the attribute value of feature j

$w_{i,j}$: spatial weight of i and j

n : number of features

$$\bar{X} = \frac{\sum_{j=1}^{n} x_j}{n} \quad \text{.....(15)}$$

$$S = \sqrt{\frac{\sum_{j=1}^{n} x_j^2}{n} - (\bar{X})^2} \quad \text{.....(16)}$$

The value of G_i^* statistics equal to z-score.

RESULTS AND DISCUSSION

LULC Changes During Study Periods

Land use land cover (LULC) data were obtained in three periods: 2013, 2017 and 2021. The LULC was classified into seven classes: Agriculture, Bareland, Built area, Forest, Garden, Shrubs and Water. The LULC types changed dramatically, but the most significant ones were Built, Bareland, Garden, and Agriculture, as shown in **Table 2** and **Figure 2**.

In summary, the built-up area increased significantly; Agriculture, Bareland, and Gardens were dynamic, while Forest remained the dominant land cover in the study area. Built-up area increased significantly from 622.25 ha (1%) in 2013 to 1,087.63 ha (2%) in 2017, and more significantly in 2021 with 4,719.63 ha (8%). The built-up area increase can not be separated from Bareland, which changed from 428.17 ha in 2013, 95.43% in 2017, and 2,265.37 ha in 2021. Bareland is often considered as land cover that is in the process of becoming a built-up area, i.e. agricultural land that is being prepared to be converted to the built area or under-construction land, and agricultural land that is dried and vacant is included in this classification.

The agricultural area experienced a slight increase from 23,086.39 ha in 2013 to 24,359.36 ha in 2017, although it decreased significantly to 15,880.74 ha in 2021. The Garden also fluctuated from 7,621.80 ha in 2013 to 5,850.86 ha in 2017 and increased to 6,939.86 ha in 2021. Gardens in this study are interpreted as vegetated areas around settlement areas; moreover this land cover is sometimes also classified as rural settlements. Sukri et al., (2021) also described that some vegetated areas in the Kulon Progo area are often converted into other LULC classes, i.e. shrubs to agriculture, and it is also possible from agricultural land to garden or forest, depending on the crop cultivation pattern and the commodities.

Figure 2 shows the distribution of LULC in Kulon Progo Regency for three points of time. Overall, the LULC distribution is related to the topographical conditions and landforms, which also stated by Roy & Das (2021) in their research. The mountainous or hilly landforms are mostly covered by forest, while built-up land and agricultural land are located in the plain area.

The Menoreh Hill, in the north and west study area, is a denudational landform, mostly covered by forest and garden. On the other hand, the urban area, which is mainly a built area, is located in the alluvial plain in the centre and south study area. Agricultural land is mainly placed in the alluvial plain on the east side and along the coastal area, especially the dry land. The water land cover is identified as water reservoir rivers and estuary.

Further analysis is needed to evaluate the LULC changes concerning Spatial Planning in the study area. Since Kulon Progo is also highly vulnerable to disasters, especially Tsunamis (Jati et al., 2023; Wicaksono et al., 2015), disaster risk reduction-based spatial planning is highly needed (Dahlia et al., 2020) since urbanization is growing rapidly in the study area.

Table 2. LULC changes from 2013, 2017 and 2021 in Kulon Progo Regency

Year		Agriculture	Bareland	Built up	Forest	Garden	Shrubs	Water
2013	hectare	23,086.39	428.17	622.25	24,786.85	7,621.80	98.19	687.78
	(%)	40.00%	1.00%	1.00%	43.00%	13.00%	0.00%	1.00%
2017	hectare	24,359.36	95.43	1,087.63	24,431.37	5,850.86	680.31	826.47
	(%)	42.00%	0.00%	2.00%	43.00%	10.00%	1.00%	1.00%
2021	hectare	15,880.74	2,265.37	4,719.63	26,071.98	6,939.86	7.7	1,446.16
	(%)	28.00%	4.00%	8.00%	45.00%	12.00%	0.00%	3.00%

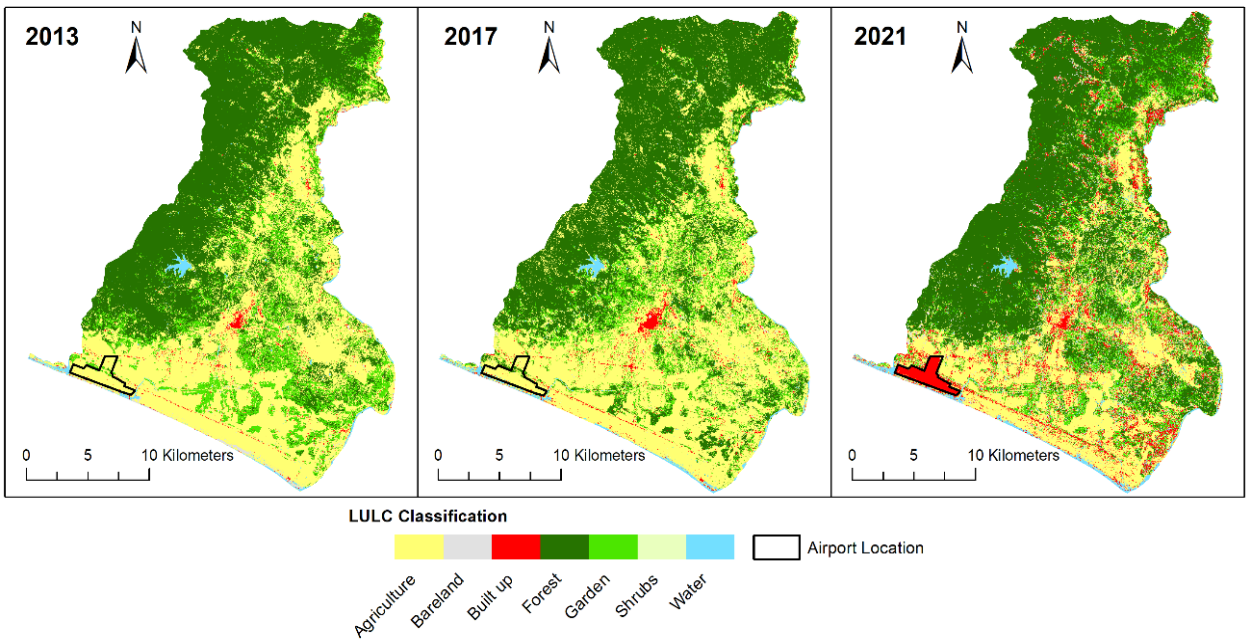

Figure 2. LULC in Kulon Progo Regency

Land Surface Temperature

Land surface temperature was estimated from Landsat 8 Imagery for three periods, i.e. before YIA development, at the start of the YIA construction and after the YIA has fully operated. The LST was the average temperature for one year or each study periods. The spatio-temporal analysis of LST is often undertaken to describe the environmental response to urbanisation or LULC change.

In summary, the trends of LST values in Kulon Progo during study periods moderately declined (**Figure 3. a**). The maximum temperature in Kulon Progo dropped significantly from 51.66 ºC to 47.15 ºC in 2017 and continued to decrease slightly to 45.74 ºC in 2021. The average LST experienced a minor dip from 33.24 ºC to 32.06 ºC and slumped to 29.58 ºC. Similarly, the minimum temperature also experienced a notable decrease, from 21.58 ºC in 2013 to 13.01 ºC in 2017. Although in 2021, it increased to 17.68 ºC, the overall trend of LST has declined over the study periods.

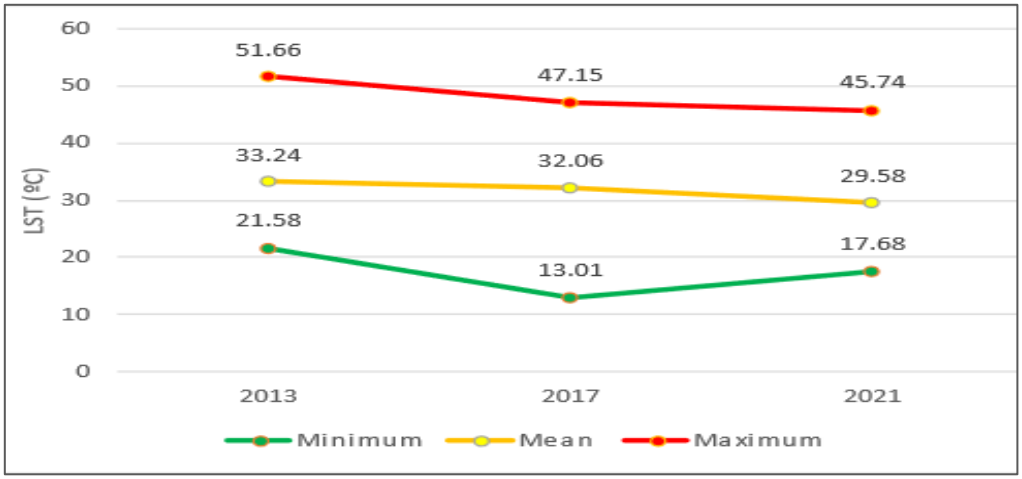

(a)

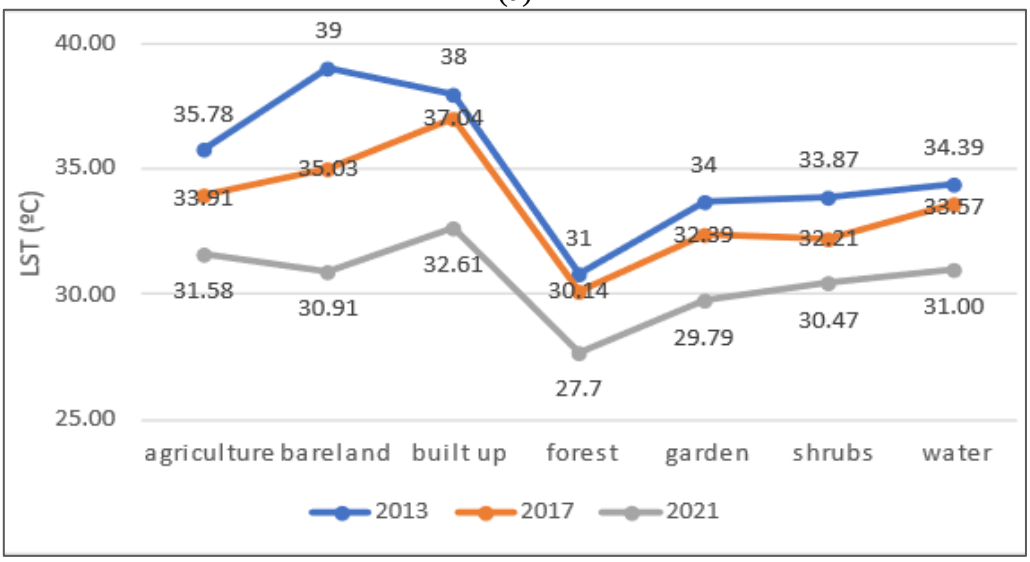

(b)

Figure 3. Land Surface Temperature (a) LST during study periods (b) The mean LST over different LULC

The LST distribution in the study area was closely related to the LULC, or LST in each LULC is significantly diverse (**Figure 3. b**). The built-up area, bare land, and agriculture mostly had higher mean temperatures than other LULCs in every period. Gardens, shrubs, and water recorded lower LST compared to the previous group of LULC, while forests still had the lowest LST in the study area over study periods. Built-up, bare land and agricultural land were considered contributed to the high LST due to the low vegetation cover (Mohammad et al., 2022; Njoku & Tenenbaum, 2022; Olorunfemi et al., 2020).

In addition, agricultural land in the study area is mainly distributed along the south coastal zone, which is dry or sandy farming land (**Figure 4**). The farmer grew horticulture products i.e., chili, watermelon, shallot, and melon which have short crop periods, (Nugroho et al., 2018; Sutardi, 2017; Yekti et al., 2019). The crops cause a lower vegetation density, contributing to the higher temperature, or in other words, the densely vegetation generally has lower LST compared to the area with sparce dense vegetation (Al Shawabkeh et al., 2023; Igun & Williams, 2018).

On the other hand, the low temperature is located on the west side or around Menoreh Hill, which has a higher elevation and is mainly covered by forest. In summary, the highly densely vegetated land cover around Menoreh Hill contributes more to lowering the LST value compared to the land cover with low vegetation density in the coastal area, which resulted in higher LST value.

Spatial statistics analysis

The spatial statistical analysis of LST distribution in the study area is obtained by analysing the Spatial Statistics Toolbox in ArcGIS, namely spatial autocorrelation (Moran's I) and Hot Spot Analysis (Getis-Ord Gi*). The LST data derived from remote sensing imagery were spatially joined with the vector grids that had identical size as the imagery pixel.

The spatial autocorrelation analysis in **Table 3** shows that Moran's Index is positive and more significant than 0.9. It indicates that there was a positive spatial autocorrelation. Furthermore, the z-score also shows that the value is more significant than 2.58, while the p-values are less than 0.05 (0.0000). These two statistical significance measurements suggest that the random assumption and data independence were ruled out. In summary, the spatial statistics insist that the LST in the study area during the study periods had positive autocorrelation. In other words, the LST distribution pattern is highly clustered.

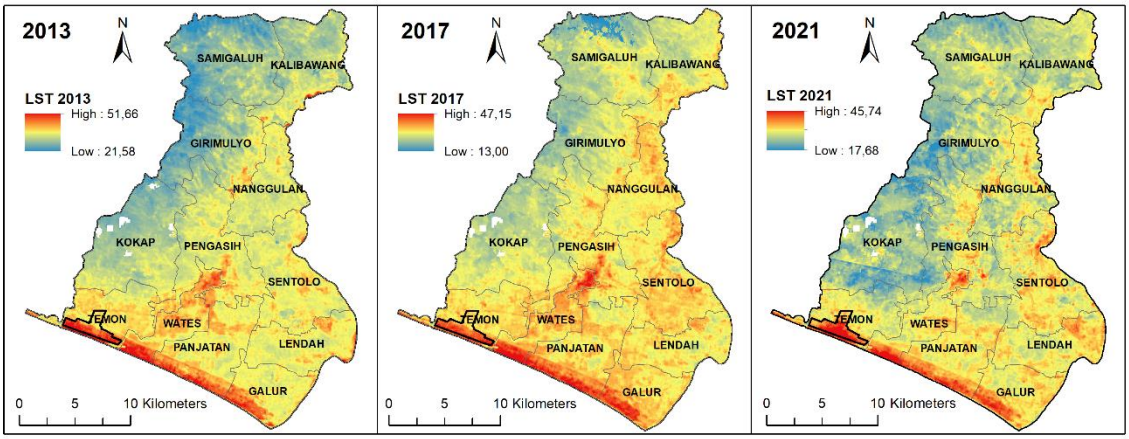

Figure 4. LST (ºC) over the study periods

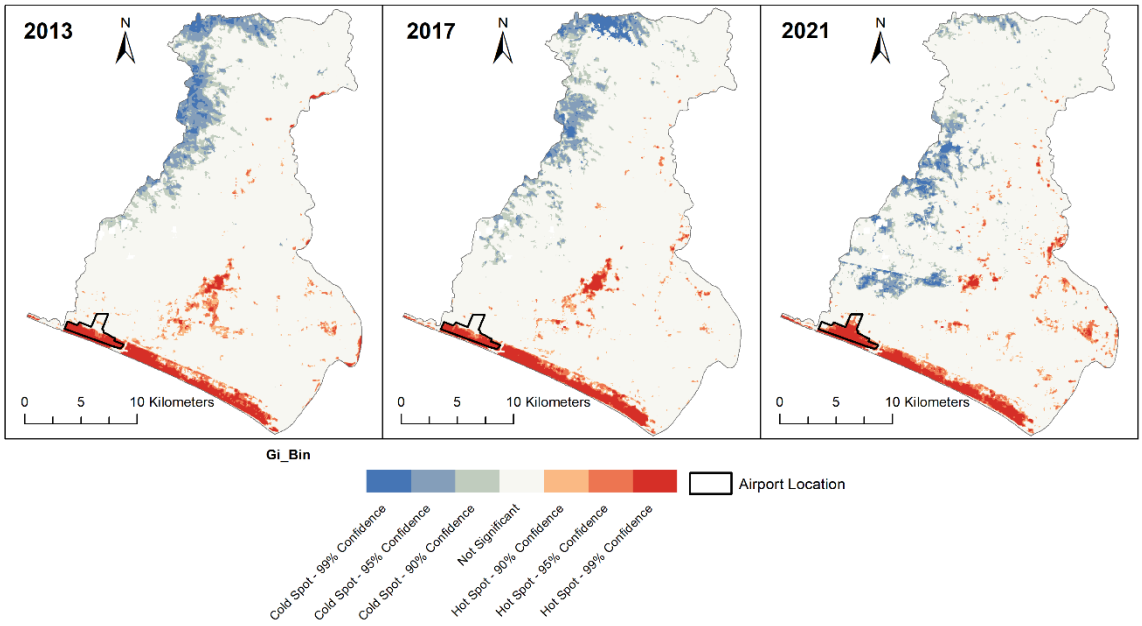

Figure 5. Hot spot analysis of LST (ºC) for three periods of time

Table 3. Global Moran's I Statistics

Year	Moran's Index	z-score	p-value
2013	0.9889	1,574.94	0.0000
2017	0.9811	1,562.98	0.0000
2021	0.9773	1,556.84	0.0000

Further analysis, namely Hot Spot Analysis (Getis-Ord Gi*), was performed to discover the spatial pattern of LST in the study area. **Figure 5** shows clusters of high-value or hot spots and low-value or cold spots. Hot spots are primarily located in the south along with coastal areas and around the urban area. On the other hand, the cold spot with the low value of LST is distributed in the west and north areas around Menoreh Hill. Overall, the spatial pattern of LST is closely related to the types LULC.

The cluster of high LST values around YIA in 2021 increased slightly compared to 2013 and 2017. The result differs from Kumari et al. (2019), where the power plant projects caused significant changes in LST and triggered clusters of high LST value. The power plant project was located around the forest area, which led to land use conversion from densely vegetated land into built-up land. On the other hand, YIA development and the newly built-up area mostly took place in predominantly sandy farming land where the LST was already high due to less dense vegetation cover.

CONCLUSIONS.

This study focuses on the impact assessment of YIA development on LULC and LST around Kulon Progo Regency, respectively: before (2013), during (2017), and after (2021) YIA development. Landsat 8 was employed to derive LULC and LST in Kulon Progo Regency in study periods. The spatiotemporal analysis presents a significant increase of built-up land and bare land (open area) around the urban area and YIA location. In contrast, agricultural land has decreased significantly since YIA construction started especially which located around the YIA and Kulon Progo's urban area.

The spatial pattern of LST has a significant relation with LULC, where the higher temperature was located in built-up areas and bare land, while the lowest temperature was in the forest. Furthermore, based on spatial statistics analysis, the spatial pattern of LST was

significantly clustered. The high temperatures (hot spots) are mainly distributed along coastal areas, primarily dry agricultural land and urban areas. On the other hand, the low temperatures (cold spots) are primarily located in the hilly areas around Menoreh Hill, which are mostly covered with dense vegetation or forest.

ACKNOWLEDGMENTS

This study was supported by the research grant from Vocational College, University of Gadjah Mada in the year 2022

REFERENCES

Al Shawabkeh, R., AlHaddad, M., Al-Fugara, A., Al-Hawwari, L., Al-Hawwari, M. I., Omoush, A., & Arar, M. (2023). Modeling the impact of urban land cover features and changes on the land surface temperature (LST): The case of Jordan. *Ain Shams Engineering Journal*, *May*, 102359. https://doi.org/10.1016/j.asej.2023.102359

Arrofiqoh, E. N., & Setyaningrum, D. A. (2021). The Impact of Covid-19 Pandemic on Land Surface Temperature in Yogyakarta Urban Agglomeration. *Journal of Applied Geospatial Information*, *5*(1), 480–485. https://doi.org/10.30871/jagi.v5i1.2784

Atianta, L. (2020). Suhu Permukaan Lahan Dan Intensitas Pemanfaatan Ruang Di Perkotaan Yogyakarta. *Jurnal Pengembangan Kota*, *8*(2), 151–162. https://doi.org/10.14710/jpk.8.2.151-162

Ayuningtyas, W. (2022). Analisis Dampak Sosial Ekonomi Pembangunan Bandar Udara Internasional Yogyakarta (YIA) Bagi Kepala Keluarga Di Desa Glagah Kulon Progo. *Journal.Upy.Ac.Id*, *6*(1), 858–865. https://journal.upy.ac.id/index.php/pkn/article/view/2642

Bamrungkhul, S., & Tanaka, T. (2022). The assessment of land suitability for urban development in the anticipated rapid urbanization area from the Belt and Road Initiative: A case study of Nong Khai City, Thailand. *Sustainable Cities and Society*, *83*, 103988. https://doi.org/10.1016/J.SCS.2022.103988

Dahlia, S. (2021). Analisis Pola Spasial Pesebaran Kasus Covid-19 Menggunakan Sistem Informasi Geografis Di DKI Jakarta. *Jurnal Geografi, Edukasi Dan Lingkungan (JGEL)*, *5*(2), 101–108. https://doi.org/10.22236/jgel.v5i2.7098

Dahlia, S., Adiputra, A., Alwin, Najiyullah, M. A., Kamzia, & Rahmadiansyah, F. K. (2020). Analisis Perubahan Penggunaan Lahan Pasca Kejadian Tsunami Tahun 2018 Sebagai Rekomendasi Tata Ruang Di Pesisir Pantai Kecamatan Panimbang, Pandeglang, Banten. *Jurnal Geografi, Edukasi Dan Lingkungan (JGEL)*, *4*(1), 8–16. https://doi.org/10.29405/jgel.v4i1.3640

EPA. (2011). Reducing Urban Heat Islands: Compendium of Strategies. In *Reducing Urban Heat Islands: Compendium of Strategies*.

ESRI. (2023a). *How Hot Spot Analysis (Getis-Ord Gi*) works*. https://pro.arcgis.com/en/pro-app/latest/tool-reference/spatial-statistics/h-how-hot-spot-analysis-getis-ord-gi-spatial-stati.htm

ESRI. (2023b). *How Spatial Autocorrelation (Global Moran's I) works*. https://pro.arcgis.com/en/pro-app/latest/tool-reference/spatial-

statistics/h-how-spatial-autocorrelation-moran-s-i-spatial-st.htm

Estoque, R. C., Murayama, Y., & Myint, S. W. (2017). Effects of landscape composition and pattern on land surface temperature: An urban heat island study in the megacities of Southeast Asia. *Science of the Total Environment*, *577*, 349–359. https://doi.org/10.1016/j.scitotenv.2016.10.195

Fischer, M. ., & Getis, A. (2010). *Handbook of Applied Spatial Analysis: Software Tools, Methods and Applications*. Springer Verlag.

RPJMD Kabupaten Kulon Progo Tahun 2017-2022, Pemerintah Kabupaten Kulon Progo 563 (2017). http://www.dof.gov.my/en/c/document_library/get_file?uuid=e25cce1e-4767-4acd-afdf-67cb926cf3c5&groupId=558715

Ha, T. V., Tuohy, M., Irwin, M., & Tuan, P. V. (2020). Monitoring and mapping rural urbanization and land use changes using Landsat data in the northeast subtropical region of Vietnam. *Egyptian Journal of Remote Sensing and Space Science*, *23*(1), 11–19. https://doi.org/10.1016/j.ejrs.2018.07.001

Igun, E., & Williams, M. (2018). Impact of urban land cover change on land surface temperature. *Global Journal of Environmental Science and Management*, *4*(1), 47–58. https://doi.org/10.22034/gjesm.2018.04.01.005

Indrawati, D. M., Suharyadi, S., & Widayani, P. (2020). Analisis Pengaruh Kerapatan Vegetasi Terhadap Suhu Permukaan dan Keterkaitannya Dengan Fenomena UHI. *Media Komunikasi Geografi*, *21*(1), 99. https://doi.org/10.23887/mkg.v21i1.24429

Jati, B. A. E. K., Akbar, M. F. Al, Wahyuni, T., Khasanah, E. U., Paramanandi, A. R. G., Sutiono, H. E. C. P., Setyaningsih, D. P., Widyatmanti, W., & Wibowo, T. W. (2023). Analysis of Tsunami Evacuation Route Planning in Kulon Progo Regency. *International Journal of Remote Sensing and Earth Sciences (IJReSES)*, *20*(1), 16. https://doi.org/10.30536/j.ijreses.2023.v20.a3823

Krishnan, P., Kochendorfer, J., Dumas, E. J., Guillevic, P. C., Baker, C. B., Meyers, T. P., & Martos, B. (2015). Comparison of in-situ, aircraft, and satellite land surface temperature measurements over a NOAA Climate Reference Network site. *Remote Sensing of Environment*, *165*, 249–264. https://doi.org/10.1016/j.rse.2015.05.011

Kumari, M., Sarma, K., & Sharma, R. (2019). Using Moran's I and GIS to study the spatial pattern of land surface temperature in relation to land use/cover around a thermal power plant in Singrauli district, Madhya Pradesh, India. *Remote Sensing Applications: Society and Environment*, *15*. https://doi.org/10.1016/j.rsase.2019.100239

Latif, M. S. (2014). Land Surface Temperature Retrival of Landsat-8 Data Using Split Window Algorithm-A Case Study of Ranchi District. *Internal Journal of Engineering Development and Research*, *2*(4), 3840–3849.

Li, W., Wang, D., Liu, S., & Zhu, Y. (2019). Measuring urbanization-occupation and internal conversion of peri-urban cultivated land to determine changes in the peri-urban agriculture of the black soil region.

Ecological Indicators, *102*, 328–337. https://doi.org/10.1016/j.ecolind.2019.02.055

Liang, J., Xie, Y., Sha, Z., & Zhou, A. (2020). Modeling urban growth sustainability in the cloud by augmenting Google Earth Engine (GEE). *Computers, Environment and Urban Systems*, *84*(March), 101542. https://doi.org/10.1016/j.compenvurbsys.2020.101542

Mohammad, P., Goswami, A., Chauhan, S., & Nayak, S. (2022). Machine learning algorithm based prediction of land use land cover and land surface temperature changes to characterize the surface urban heat island phenomena over Ahmedabad city, India. *Urban Climate*, *42*(July 2021), 101116. https://doi.org/10.1016/j.uclim.2022.101116

Naikoo, M. W., Rihan, M., Ishtiaque, M., & Shahfahad. (2020). Analyses of land use land cover (LULC) change and built-up expansion in the suburb of a metropolitan city: Spatio-temporal analysis of Delhi NCR using landsat datasets. *Journal of Urban Management*, *9*(3), 347–359. https://doi.org/10.1016/j.jum.2020.05.004

Nando, F. H. (2021). Perubahan Kondisi Variasi Land Surface Temperature di Masa Pandemi Covid-19 (Studi Kasus: Kota Kediri, Jawa Timur). *Jurnal Geografi, Edukasi Dan Lingkungan (JGEL)*, *5*(2), 92–100. https://doi.org/10.22236/jgel.v5i2.7032

Njoku, E. A., & Tenenbaum, D. E. (2022). Quantitative assessment of the relationship between land use/land cover (LULC), topographic elevation and land surface temperature (LST) in Ilorin, Nigeria. *Remote Sensing Applications: Society and Environment*, *27*, 100780. https://doi.org/10.1016/j.rsase.2022.100780

Nugraha, Gunawan, T., & Kamal, M. (2019). Comparison of Land Surface Temperature Derived from Landsat 7 ETM+ and Landsat 8 OLI/TIRS for Drought Monitoring. *IOP Conference Series: Earth and Environmental Science*, *313*(1). https://doi.org/10.1088/1755-1315/313/1/012041

Nugraha, I. C., Siti Fatimah, Belia Fransiska, & Endriana Prasetyawati. (2022). Bela Beli Kulon Progo Sebagai Sebuah Model Endogenous Development. *Jurnal Litbang Sukowati : Media Penelitian Dan Pengembangan*, *6*(1), 123–140. https://doi.org/10.32630/sukowati.v6i1.333

Nugroho, A. D., Prasada, I. M. Y., Putri, S. K., Anggrasari, H., & Sari, P. N. (2018). Rantai Nilai Cabai di Lahan Pasir Pantai Kabupaten Kulon Progo. *Economics Development Analysis Journal*, *7*(4), 458–467. https://doi.org/10.15294/edaj.v7i4.25013

Ochoa, J. J., Tan, Y., Qian, Q. K., Shen, L., & Moreno, E. L. (2018). Learning from best practices in sustainable urbanization. *Habitat International*, *78*, 83–95. https://doi.org/10.1016/J.HABITATINT.2018.05.013

Olorunfemi, I. E., Fasinmirin, J. T., Olufayo, A. A., & Komolafe, A. A. (2020). GIS and remote sensing-based analysis of the impacts of land use/land cover change (LULCC) on the environmental sustainability of Ekiti State, southwestern Nigeria. *Environment, Development and Sustainability*, *22*(2), 661–692. https://doi.org/10.1007/s10668-018-0214-z

Pradhan, B., Al-sharif, A. A. A., & Abdullahi, S. (2017). Urban sprawl

assessment. In *Spatial Modeling and Assessment of Urban Form: Analysis of Urban Growth: From Sprawl to Compact Using Geospatial Data*. https://doi.org/10.1007/978-3-319-54217-1_4

Prastyo, F. U., Nurjani, E., & Giyarsih, S. R. (2022). Distribusi Spasial Surface Urban Heat Island (SUHI) Kawasan Permukiman Perkotaan di Kota Yogyakarta. *Media Komunikasi Geografi*, *23*(1), 73–83. https://doi.org/10.23887/mkg.v23i1.34300

Pratiwi, R. D., Fatimah, I. S., & Munandar, A. (2018). Spatial planning for green infrastructure in Yogyakarta City based on land surface temperature. *IOP Conference Series: Earth and Environmental Science*, *179*(1). https://doi.org/10.1088/1755-1315/179/1/012004

Punzo, G., Castellano, R., & Bruno, E. (2022). Using geographically weighted regressions to explore spatial heterogeneity of land use influencing factors in Campania (Southern Italy). *Land Use Policy*, *112*(September 2021), 105853. https://doi.org/10.1016/j.landusepol.2021.105853

Roy, L., & Das, S. (2021). GIS-based landform and LULC classifications in the Sub-Himalayan Kaljani Basin: Special reference to 2016 Flood. *Egyptian Journal of Remote Sensing and Space Science*, *24*(3), 755–767. https://doi.org/10.1016/j.ejrs.2021.06.005

Rustiadi, E., Pravitasari, A. E., Setiawan, Y., Mulya, S. P., Pribadi, D. O., & Tsutsumida, N. (2021). Impact of continuous Jakarta megacity urban expansion on the formation of the Jakarta-Bandung conurbation over the rice farm regions. *Cities*, *111*, 103000. https://doi.org/10.1016/j.cities.2020.103000

Sam, S. C., & Balasubramanian, G. (2023). Spatiotemporal detection of land use/land cover changes and land surface temperature using Landsat and MODIS data across the coastal Kanyakumari district, India. *Geodesy and Geodynamics*, *14*(2), 172–181. https://doi.org/10.1016/j.geog.2022.09.002

Saputra, M. H., & Lee, H. S. (2019). Prediction of land use and land cover changes for North Sumatra, Indonesia, using an artificial-neural-network-based cellular automaton. *Sustainability (Switzerland)*, *11*(11), 1–16. https://doi.org/10.3390/su11113024

Singh, P., Kikon, N., & Verma, P. (2017). Impact of land use change and urbanization on urban heat island in Lucknow city, Central India. A remote sensing based estimate. *Sustainable Cities and Society*, *32*, 100–114. https://doi.org/10.1016/j.scs.2017.02.018

Statistical Bureau of Kulon Progo Regency. (2023). *Kulon Progo Dalam Angka Tahun 2023*.

Sukri, I., Harini, R., & Sudrajat. (2021). Analisis Perubahan Penggunaan Lahan di Kabupaten Kulon Progo Menggunakan Citra Landsat 7 Tahun 2011 dan Landsat 8 Tahun 2019. *Seminar Nasional Geografi IV Magister Geografi UGM.*, *September*, 255–263.

Sutardi. (2017). Kajian Minus One Test Dan Kesuburan Lahan Pasir Untuk Budidaya Tanaman Bawang Merah. *Jurnal Pengkajian Dan Pengembangan Teknologi Pertanian*, *20*(22), 25–34.

Wicaksono, D., Ardiansyah, F., Nugroho, G. A., & S, C. A. T. (2015). Analisis Multi-Skenario Dampak Tsunami Di Kawasan Pesisir Kabupaten Kulon

Progo ,. *Pertemuan Ilmiah Tahunan (PIT) Ke-2 Ikatan Ahli Kebencanaan Indonesia*, *1*.

Widodo, B., Lupyanto, R., Sulistiono, B., Harjito, D. A., Hamidin, J., Hapsari, E., Yasin, M., & Ellinda, C. (2015). Analysis of Environmental Carrying Capacity for the Development of Sustainable Settlement in Yogyakarta Urban Area. *Procedia Environmental Sciences*, *28*(SustaiN 2014), 519–527. https://doi.org/10.1016/j.proenv.2015.07.062

Yekti, A., Darwanto, D. H., Jamhari, J., & Hartono, S. (2019). Strategi Manajemen Risiko Usahatani Melon Di Lahan Pasir Pantai Kabupaten Kulon Progo. *Jurnal Ilmu-Ilmu Pertanian*, *26*(1), 51–63. https://doi.org/10.55259/jiip.v26i1.208

Zoomers, E. B. (Annelies., & Otsuki, K. (2017). Addressing the impacts of large-scale land investments: Re-engaging with livelihood research. *Geoforum*, *83*, 164–171. https://doi.org/10.1016/J.GEOFORUM.2017.01.009